PRECISE ORBIT DETERMINATION OF THE GOCE RE-ENTRY PHASE

Francesco Gini[1], Michiel Otten[2], Tim Springer[2], Werner Enderle[1], Stijn Lemmens[3], and Tim Flohrer[4]

[1]*ESA/ESOC Navigation Support Office (HSO-GN)*
[2]*PosiTim at ESA/ESOC Navigation Support Office (HSO-GN)*
[3]*IMS Space Consultancy GmbH at ESA/ESOC Space Debris Office (HSO-GR)*
[4]*ESA/ESOC Space Debris Office (HSO-GR)*

ABSTRACT

During the last days of the GOCE mission, after the GOCE spacecraft ran out of fuel, it slowly decayed before finally re-entering the atmosphere on the 11th November 2013. As an integrated part of the AOCS, GOCE carried a GPS receiver that was in operations during the re-entry phase. This feature provided a unique opportunity for Precise Orbit Determination (POD) analysis. As part of the activities carried out by the Navigation Support Office (HSO-GN) at ESOC, precise ephemerides of the GOCE satellite have been reconstructed for the entire re-entry phase based on the available GPS observations of the on-board LAGRANGE receiver. All the data available from the moment the thruster was switched off on the 21st of October 2013 to the last available telemetry downlink on the 10th November 2013 have been processed, for a total of 21 daily arcs. For this period a dedicated processing sequence has been defined and implemented within the ESA/ESOC NAvigation Package for Earth Observation Satellites (NAPEOS) software.

The computed results show a post-fit RMS of the GPS undifferenced carrier phase residuals (ionospheric-free linear combination) between 6 and 14 mm for the first 16 days which then progressively increases up to about 80 mm for the last available days. An orbit comparison with the Precise Science Orbits (PSO) generated at the Astronomical Institute of the University of Bern (AIUB, Bern, Switzerland) shows an average difference around 9 cm for the first 8 daily arcs and progressively increasing up to 17 cm for the following days.

During this reentry phase (21st of October - 10th November 2013) a substantial drop in the GOCE altitude is observed, starting from about 230 km to 130 km where the last GPS measurements were taken. During this orbital decay an increment of a factor of 100 in the aerodynamic acceleration profile is observed. In order to limit the mis-modelling of the non-gravitational forces (radiation pressure and aerodynamic effects) the newly developed software ARPA (Aerodynamics and Radiation Pressure Analysis) has been adopted to compute the forces acting on GOCE. An overview of the software techniques and the results of its implementation is presented in this paper. The use of the ARPA modelling leads to an average reduction of the carrier phase post-fit RMS of about 2 mm and decrement of the difference with the PSO orbits of more than 1 cm.

Key words: GOCE; reentry; POD; NAPEOS; ARPA.

1. INTRODUCTION

The Gravity field and steady-state Ocean Circulation Explorer is the first Earth explorer core mission of the European Space Agency (ESA). It was launched on 17 March 2009 and its science phase covered the time interval between the 1st of November 2009 to 21st October 2013. During this period the satellite was flying in a drag-free mode. On the 21st of October 2013 the spacecraft ran out of fuel and the thruster was switched off, starting its orbital decay.

The GPS data available for the reentry phase have been processed with the ESA/ESOC NAPEOS software. A sequence of programs has been defined and implemented to process the data and estimate the daily orbital arcs. An overview of the implemented sequence is described in the first section. In the second paragraph an overview of the data used for the GOCE reentry POD is given.

At an extremely low altitude between 230 km and 130 km (altitudes at which the GPS data were successfully downlinked) the main non-gravitational perturbation was the atmospheric drag. In order to accurately describe the interaction of the spacecraft with the atmospheric particles the software ARPA has been used to compute the non-gravitational forces acting on GOCE. In this paper an overview of the approach and models adopted in this software is given in the third section. The impact of this sophisticated modelling on the POD results is presented in the results section.

The dynamical model adopted for the orbit determination is described in the fourth paragraph.

All the 21 days of data have been processed and precise ephemerides of the satellite has been reconstructed. In

Proc. '5th International GOCE User Workshop', Paris, France 25–28 November 2014 (ESA SP-728, March 2015)

the fifth section the results obtained with the standard NAPEOS models and the ARPA models are presented and discussed, and the computed orbits are then compared with the Official Precise Science Orbits (PSO).

Conclusions are then reported to summarize the results.

2. GNSS PROCESSING STEPS FOR THE REENTRY PHASE POD

The undifferenced GPS observations available from the GOCE on-board receiver have been processed based on a fully-dynamic approach, by using the ionospheric-free linear combination. A NAPEOS sequence of programs has been set up to perform the GOCE reentry POD. In addition to the GPS observations from the on-board receiver other input files required for the processing are the IGS final products (ephemerides and clocks).

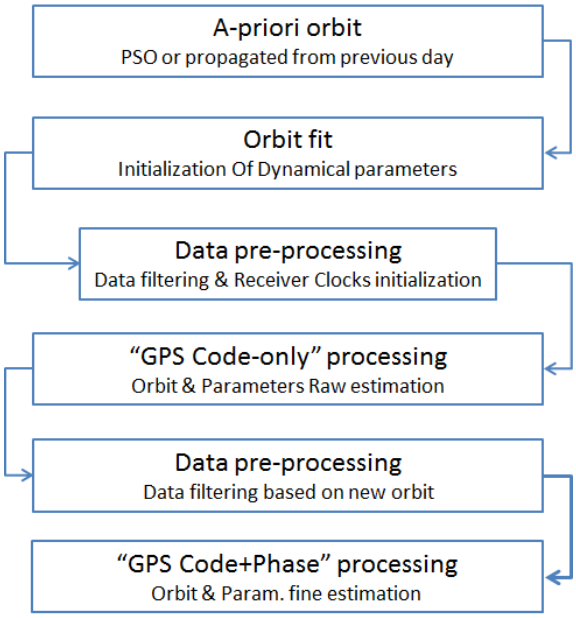

Figure 1. Sequence of steps performed for the GOCE precise orbit determination.

Figure 1 shows the sequence of steps performed for the GOCE precise orbit determination. To start the sequence an a-priori orbit was necessary to initialize GOCE's ephemerides and parameters. For the first day, 21st October 2013, the PSO was used. For the initialization of the following days, the daily arc propagated from the previous day has been used instead. An orbit fit of the positions from the a-priori orbit is then performed with the selected dynamical model that will be later described. This step is used to initialize the dynamical parameters. As a further step the GPS data are pre-processed based on the fitted orbit, in order to filter the observations and initialize the receiver clocks. After this step an initial orbit determination is performed, processing only the GPS code. This allows a better initialization of the dynamical parameters and initial state. A meter-level a-priori orbit is also computed as input for the following steps. The GPS data are then pre-processed again based on the new a-priori orbit, filtering the available observations. As a last step the GPS code and carrier-phase data are processed in order to compute the best accurate orbit and parameters.

3. GOCE REENTRY DATA USED FOR POD

GOCE POD has been performed using as main input the raw GPS code and phase observables from the on-board 12-channel dual-frequency LAGRANGE (Laben GNSS Receiver for Advanced Navigation, Geodesy and Experiments) receiver, freely downloadable in RINEX 2.20 format. These data cover the period of time from the 21st of October 2013 at about 04:04 to the 10th November 2013 at about 17:15, for a total of 19 complete days and 2 partial days of observations, as shown in Figure 2.

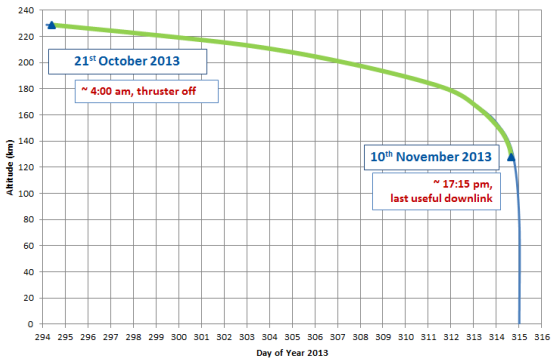

Figure 2. Altitude profile along the reentry, showing in green the arc with GPS data availability.

International GNSS Service (IGS) final GPS orbits and clock solutions were also retrieved for the processed days.

Official GOCE reduced-dynamic PSO solutions, generated at the Astronomical Institute of the University of Bern (AIUB, Bern, Switzerland) with the support of the Institute of Astronomical and Physical Geodesy (IAPG, Technische Universität München, München, Germany) [3, 14], have been used for two reasons: 1) to initialize the sequence of programs as a-priori orbit and 2) as term of comparison with the determined orbits. The PSO solutions are available for the first 16 days of the reentry phase, from the 21st of October 2013 to the 5th of November 2013. At the End Of Life (EOL), when all the fuel was consumed, the position of the center of mass and the mass of the satellite itself were different from the Beginning Of Life (BOL) conditions, and needed to be updated, as in ESA [6]. Precise position of the GPS antenna was also required, in terms of antenna Center of Mounting Plane (CMP) with respect to the satellite CoM

[2], antenna Phase Center Offsets (PCOs) and Phase Center Variations (PCVs), these last two both provided in ANTEX (ANTenna EXchange) format for the L1 and L2 frequencies in an antenna-fixed reference frame [5, 9].

In order to accurately model the non-gravitational forces acting on GOCE by means of the software ARPA, other data related to the satellite geometry and surface properties has been necessary, (i.e, optical and thermal properties, temperatures, surface material).

In addition to the previously described parameters, an accurate knowledge of satellite attitude during the reentry is fundamental for the correct modelling of the non-gravitational forces and for the correct positioning of the GPS antenna along the orbit. Figure 3 shows the two main GOCE reference frames: the body-fixed reference frame (b) and the local orbital frame (LORF). Based on the yaw steering law the X_b axis is maintained aligned with the velocity of the satellite relative to the winds, while the X_{LORF} axis is aligned with the absolute velocity. The the Y_{LORF} axis is orthogonal to the orbital plane and pointing positively in the same direction of the orbit angular momentum. Figure 4 shows the angles between these two reference frames.

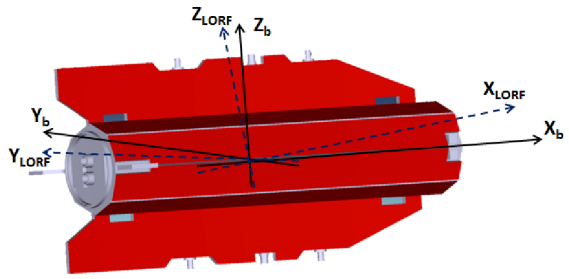

Figure 3. GOCE body-fixed (b) and local orbital frame (LORF).

During the reentry phase, the attitude is no more as stable as it was during the drag-free mode, sometimes showing significant deviations from the nominal attitude, as shown in Figure 4.

4. ARPA NON-GRAVITATIONAL FORCES MODELLING

The *Aerodynamics and Radiation Pressure Analysis* – ARPA – software is the tool designed and implemented at the University of Padova and upgraded at ESA, to compute forces and torques on satellites due to the non-gravitational perturbations: Solar Radiation Pressure (SRP), Earth Radiation Pressure (ERP) for the albedo and infrared components, the satellite Thermal Re-Radiation (TRR), and the aerodynamics. Here an overview of the ARPA software and model is presented, and for a more

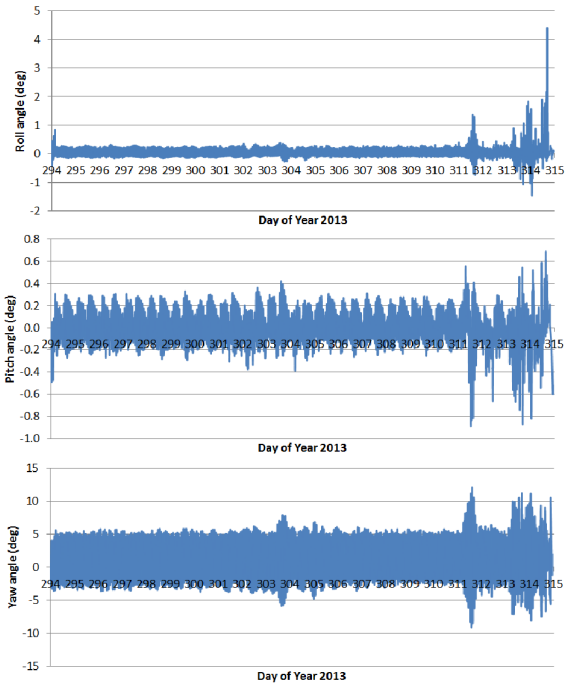

Figure 4. GOCE Euler angles for the entire reentry period, as a function of time (day of the year 2013). The Euler angles are computed with respect to the local orbital frame.

detailed description the reader is referred to Gini et al. [8].

For all the components of forces computed by ARPA an accurate geometry is required, and hence a CAD model of GOCE has been realized and is shown in Figure 5.

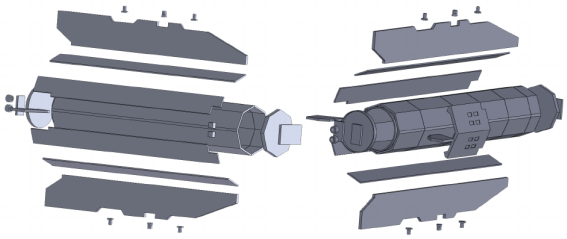

Figure 5. Exploded view of the CAD model of GOCE and its external components.

For the Solar (SRP) and Earth Radiation Pressure (ERP) the CAD model is the input for the raytracing tool, which simulates the interaction of the photons coming from the Sun or the Earth with the satellite surfaces, a shown in Figure 6. By means of the ARPA raytracing program, the ray source is located in a grid of positions to simulate all the possible directions of the incoming radiation and for each location a raytracing file is created containing all the reflection points of each traced ray. In a second step,

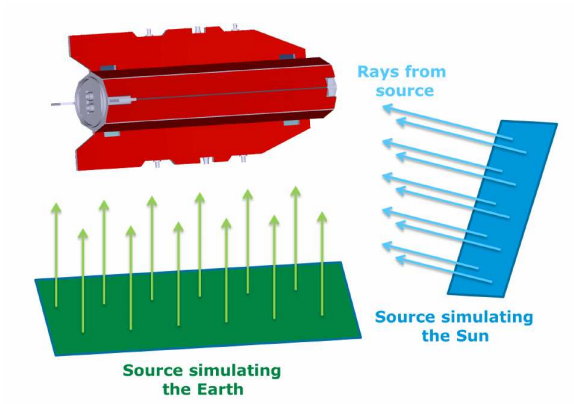

Figure 6. Raytracing procedure over GOCE. Ray sources simulating Sun and Earth are shown.

by means of the ARPA SRP/ERP software the *geometric information* contained in the raytracing files is converted into a *physical interaction*, computing forces and torques due to the radiation pressure, based on the models described by Ziebart [15]. With this photons-surface interaction description, an accurate modelling of these force components is achieved. The computed forces are collected in a database (look up tables) and are used as input for the POD process, after scaling the computed force, if necessary, to absorb eventual mismodelling.

For the Thermal Re-Radiation (TRR) force component a discretization of the satellite external surfaces have been realized, as shown in Figure 7. Based on the geometrical

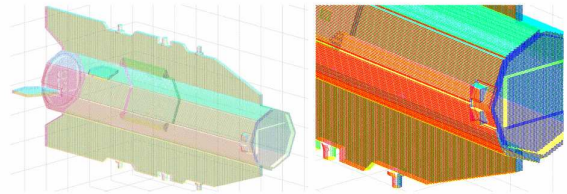

Figure 7. GOCE external surfaces meshed with pixels. Colors are used just to make the mesh clearer. On the left-hand side the entire satellite, and on the right-hand side a detail of the frontal floor.

mesh and the thermal properties and temperatures (average temperatures for the eclipsing and non-eclipsing conditions) of the surfaces, the ARPA TRR program computes the forces and torques induced on GOCE by the thermal emission. Again the forces are collected in a database and used in the POD process.

Similarly, for the satellite aerodynamics, the mesh of Figure 7 is used. By means of the ARPA aerodynamic software the interaction of the atmospheric properties with the satellite surfaces are modelled, based on the thermal free-molecular flow formulation from Pilinski et al. [12], and the forces and torques acting on the satellite are computed. Also in this case the forces are collected in a database and used in the POD process. In the NAPEOS orbit estimator (*Bahn* program) a scaling coefficient is set up for the ARPA aerodynamic forces, in order to absorb the eventual mismodelling in the aerodynamic and atmospheric models.

5. DYNAMICAL MODEL

The dynamical model adopted in the orbit determination process for the reentry phase is shown in Table 1. For the modelling of the non-gravitational forces two models have been adopted and compared: the NAPEOS standard model, which simplifies the satellite's complex surfaces to one single flat plate, and the ARPA models, which maintain a high level of accuracy of the geometry and the properties of the spacecraft. For the computation of the aerodynamic perturbations, 100 C_D's (drag coefficient scaling factor) have been set up and estimated during the POD process, in order to absorb the mismodelling of the force and atmospheric models. Similarly, 24 CPR's in the along- and cross-track directions, with the sine, cosine and constant terms, are estimated to absorb the unmodelled effects. The choice of 100 C_D's and 24 CPR's was made in order to reduce the mismodelling and hence the residuals of the GPS observations, scaling if needed the computed accelerations mainly due to the aerodynamics. This combination of parameters was selected after different tests, as the best trade-off between accuracy of the solution and convergence of the POD process for all the reentry daily arcs. At these extremely low altitudes (between 230 km and 130 km) the aerodynamics becomes significant and also the effects of the atmospheric density mismodellings, which need to be absorbed by the estimated parameters.

The dynamical model adopted for the reentry phase is significantly different from the one adopted for the drag-free phase, where no drag coefficients were necessary since the satellite was virtually experiencing no drag. Also in that case the empirical accelerations were estimated to absorb eventual mismodellings.

When testing different parametrization for the reentry phase POD, it was observed that a larger number of C_D's or CPR's, was leading to non-convergence of the POD iteration process, not allowing to estimate the final orbit and parameters. In the end the dynamical models from Table 1 was selected as the best compromise between the number of estimated parameters and the convergence and accuracy of the POD process. The dynamical model shown in Table Table 1 has been used for all the days of the reentry phase.

6. RESULTS

The sequence of programs implemented in NAPEOS was run for all the 21 arcs of the reentry phase. The first 20 arcs were computed with both the NAPEOS and ARPA

Table 1. Dynamical models: gravitational, non-gravitational and empirical forces adopted for the GOCE reentry POD. Non-gravitational and empirical estimated parameters are also shown.

Dynamical models	Description	Model	Daily Estim. Params.
Static gravity field	EIGEN-6C 200x200	[7]	
Solid Earth tides	IERS-TN32 71 constit., 3x3	[11]	
Ocean tides	FES2004 106 constit., 50x50	[10]	
Third body perturbation	Lunar gravity		
	Solar gravity		
	Planetary gravity		
	Indirect oblateness perturb.		
Relativistic correction	Correction for Gen. Relativity	[11]	
Aerodynamics	Drag force	NAPEOS[4] & ARPA[8]	100 C_D
Radiation Pressure	SRP	NAPEOS[11] & ARPA[8]	
	Albedo ERP	NAPEOS[1] & ARPA[8]	
	Infrared ERP	NAPEOS[1] & ARPA[8]	
	TRR	ARPA[8]	
Empirical accelerations	CPR along- and cross-track	[13]	24 x3 (sin., cos., const.)

non-gravitational models. For the last day the sequence based on the NAPEOS non-gravitational model has not reached the convergence leading to a non-converge of the POD estimation process, while the same sequence based on the ARPA model successfully converged (even if with a high post-fit RMS). In total 21 daily arcs have been recovered, the first arc of 20 hours, 19 arcs of 24 hours, and the last of 17 hours.

Figure 8 shows the behaviour of the undifferenced carrier-phase post-fit RMS as a function of time. As can be observed the first 16 days show a post-fit RMS between 6 and 14 mm, which then progressively increases up to about about 80 mm for the last days, with both the NAPEOS and ARPA non-gravitational models. This can be explained by the fact that for the first days of the reentry phase, the altitude was about 230 km, slowly descending due to the aerodynamic drag. At this point the aerodynamic forces, even if significant, are not as intense as at the end of the reentry, and the aerodynamic model can adequately absorb these effects. During the descending of the spacecraft the aerodynamic forces grow exponentially, even causing instabilities in the attitude of the satellite. At this point, where the attitude is no more stable and the aerodynamic effects are extremely high it becomes evident that the dynamical models implemented in NAPEOS are no more capable of accurately matching the observations, leaving high residuals. Mismodelling of the non-gravitational forces and of the adopted atmospheric model (MSIS-90) play a significant role in the high residuals.

Figure 8 also compares the NAPEOS and ARPA non-gravitational force models. The ARPA models (especially the aerodynamic one) shows an average reduction of the post-fit RMS of about 2 mm (mean value, about 15%), with differences ranging from 0.5 mm up to 6.9 mm for all the daily arcs, demonstrating the significant improvements of the solution with an accurate non-gravitational forces modelling.

The improvement of ARPA with respect to the NAPEOS

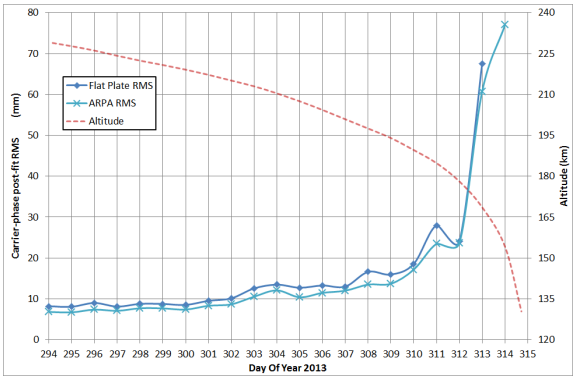

Figure 8. Post-fit RMS of undifferenced carrier phases (in millimetres) for the solutions using the NAPEOS or ARPA non-gravitational force models. Satellite altitude decay is also shown.

flat plate models can also be observed in the estimated empirical accelerations in the along-track direction, as shown in Figures 9 and 10, with a reduction of more than 20%. The cross-track CPR's components (not illustrated) show a reduction of more than the 40%. The estimated along-track CPR's (constant, sine and cosine terms), as well as the cross-track components, show lower values at the beginning of the reentry, while at the end they show much higher oscillations to absorb the unmodelled effects, mainly due to the aerodynamics.

Figures 11 shows the estimated drag coefficients (100 per day) when using the NAPEOS flat-plate aerodynamic model. It is possible to observe that since the beginning the oscillation of this parameter is high (mainly between 1.2 and 5) to absorb the effects of the aerodynamic drag. The parameter shows higher values on the days of the year 311 and 313, and this is mainly due to instabilities in the attitude of the satellite (see Figure 4). A constant area flat-plate in these conditions, where the satellite is not perfectly oriented with the velocity vector, is not ca-

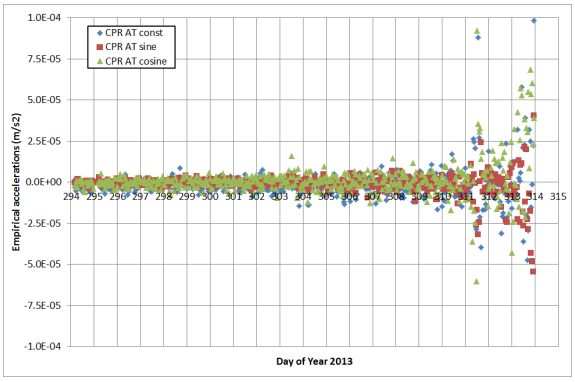

Figure 9. Estimated along-track CPR for the solution using the NAPEOS non-gravitational force models.

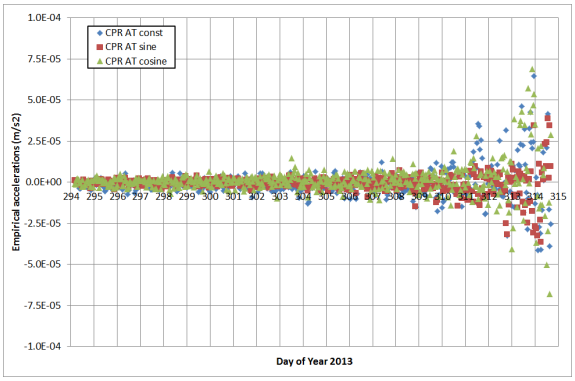

Figure 10. Estimated along-track CPR for the solution using the ARPA non-gravitational force models.

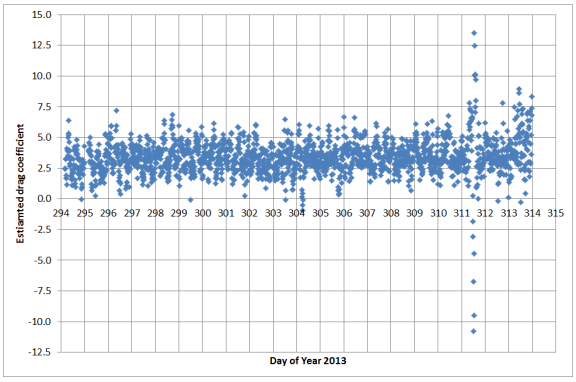

Figure 11. Estimated drag coefficients for the solution using the NAPEOS non-gravitational force models.

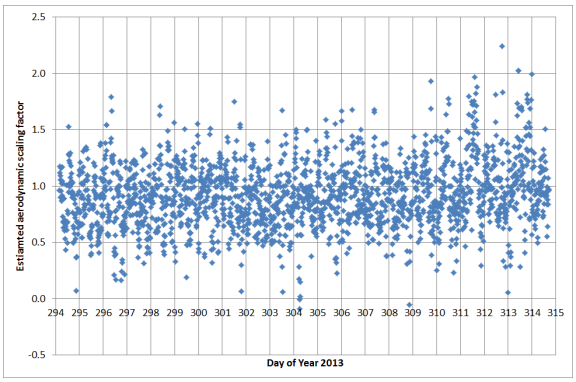

Figure 12. Estimated aerodynamic scaling factor for the solution using the ARPA non-gravitational force models.

pable of accurately modelling the variations of the GOCE projected area along the wind vector (the ratio between the satellite frontal and side area is about 11).

When the ARPA non-gravitational models are applied, the computed aerodynamic forces are scaled to better fit the observations. Figure 12 shows the estimated scaling factors (100 per day) for all the 21 daily arcs. As can be observed the values are centered around the unitary value, and most of the factors are within the range 0.5 - 1.3. For the last days, again especially for the days of year 311 and 313, the estimated values are still slightly higher, but less significantly than with the flat-plate model. This is due to the better modelling of the satellite geometry and interaction with the airflow, also in case of unstable attitude conditions. The estimated aerodynamic scaling factors show a mean value of about 0.92 with a standard deviation of less than 0.3. This shows that the aerodynamic accelerations computed with the ARPA model, when using the MSIS-90 atmospheric model, have a higher intensity than expected, by about the 8% (mean value).

As can be observed in Figure 13 the aerodynamic forces, as computed with the ARPA model and the MSIS-90 atmospheric model, show quickly increasing values as the altitude of the satellite decreases. The trend is almost exponential, showing, at the end of the available period of data, values of more than $7.E-4\ m/s^2$, which is almost 100 times higher than during the beginning of the reentry.

As a validation of the procedure adopted to recover the orbits during the reentry, the computed ephemerides where compared to the PSO's and the result is shown in Figure 14. The PSO's are available until the 5th of November 2013 (Day of Year 309). As can be observed the difference between the PSO's and the solutions computed with the NAPEOS model is set around 10 cm for the first 8 days, while with the ARPA model, for the same period, it is around 9 cm. Starting on the 29th of October (Day of Year 302) the difference becomes higher, with a quick difference jump on the DOY 303, reaching the level of about 17 cm for the last day. On the DOY 303 an attitude instability takes place, especially in the yaw angle (see Figure 4). This is even more evident in the comparison between the ARPA and NAPEOS orbits, which show an average difference of about 4.8 cm, which on the Day of Year 303 shows a jump to about 7.5 cm. This is due to the fact that the aerodynamic flat-plate model does not model all the surfaces of the satellite during the attitude changes, while ARPA is capable of accurately modelling this effect.

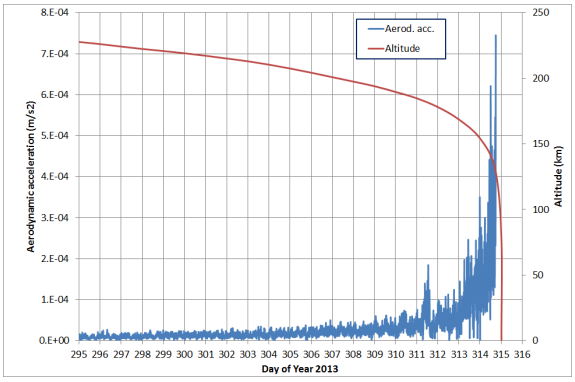

Figure 13. Evolution of the satellite aerodynamic forces and altitude as a function of time.

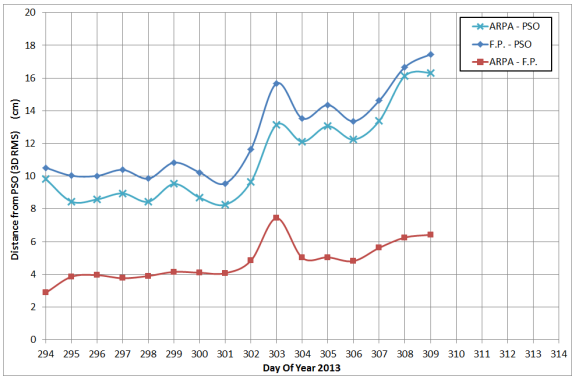

Figure 14. The 3D orbit difference RMS with respect to the reduced-dynamic PSO solutions (in centimetres).

7. CONCLUSIONS

The GPS data of the GOCE on-board LAGRANGE receiver were successfully processed and daily orbital arcs were recovered for all the observed period of the reentry phase, for a total of 21 daily arcs. It has also been possible to further test the ARPA software and its computed non-gravitational forces during the non-drag-free reentry, demonstrating its improvements on the POD solutions.

The post-fit RMS of the undifferenced carrier phase residuals shows values between 6 and 14 mm for the first 16 daily arcs, which then increase with the decrement of the orbit altitude, reaching a level of about 80 mm on the last available day, where the altitude is about 130 km.

The estimated empirical accelerations show higher values at the end of the observed reentry, as the altitude of the satellite decreases and the aerodynamic forces get higher. With the ARPA modelling a reduction of these empirical accelerations is observed, with an average decrement of about 20% in the along-track and 40% in the cross-track directions.

While the NAPEOS aerodynamic model (flat-plate) does not take into account all the satellite surfaces,their properties and their interaction with the airflow, as demonstrated by the high oscillation of the estimated drag coefficients, the ARPA model significantly reduces this mismodelling. During the reentry it was observed that the forces computed by ARPA when using the MSIS-90 atmospheric model are overestimated by about the 8%, based on the estimated aerodynamic scaling factors.

The computed final orbits were compared to the Precise Science Orbits, showing a progressively increasing difference as the altitude decreases. The orbits based on the NAPEOS models show a difference of about 10 cm for the first 8 days, while ARPA shows a value of about 9 cm. For both the models a quick jump in the orbital difference is visible for the following days, reaching a value of about 17 cm for the last available PSO. An average difference between the ARPA and NAPEOS solutions of about 5 cm has been computed, showing the significant difference between the two modelling approaches. At this point, it is not possible to state which is the most precise orbit.

REFERENCES

[1] Arnold S.J. and Dow J.M.; 1984: *Models for spacecraft acceleration due to earth albedo and infrared radiation*. OAD WP n. 265.

[2] Bigazzi A. and Frommknecht B. , *Note on GOCE instruments positioning*, tech. rep., ESA/ESRIN, 2010. 09-0007.

[3] Bock H., Jäggi A., Svehla D., Beutler G., Hugentobler U. and Visser P.N.A.M.; 2007: *Precise orbit determination for the GOCE satellite using GPS.* Adv. Space Res., 39, 1638-1647, doi:10.1016/j.asr.2007.02.053

[4] Carrou J.-P., *Spaceflight dynamics*. Cèpaduès-éd., 1995.

[5] ESA, *SSTI A/B Antenna Phase Center Variations (ANTEX)* available at `https://earth.esa.int/web/guest/missions/esa-operational-eo-missions/goce/ssti-ab-antex`

[6] ESA, *GOCE Mass Property file* available at `https://earth.esa.int/web/guest/-/goce-mass-property-file-8276`

[7] Förste C., Bruinsma S., Shako R., Marty J.-C., Flechtner F., Abrikosov O., Dahle C., Lemoine J.-M., Neumayer K.H., Biancale R., Barthelmes F., König R. and Balmino G.; 2011: *EIGEN-6 - A new combined global gravity field model including GOCE data from the collaboration of GFZ-Potsdam and GRGS-Toulouse*. In: Proc. General Res. Eur. Geosci. Union, Vienna, Austria, Geophys. Res. Abstr. Vol. 13, EGU2011-3242-2.

[8] Gini F., Bardella M., Casotto S.; 2014: *Precise Non-Gravitational Forces modelling for GOCE*, Advances in the Astronautical Sciences Spaceflight Mechanics Volume 152

[9] Jäggi A., Dach R., Montenbruck O., Hugentobler U., Bock H., and Beutler G., *Phase center modelling for LEO GPS receiver antennas and its impact on precise orbit determination*, Journal of geodesy, Vol. DOI 10.1007/s00190-009-0333-2, No. 83, 2009, pp. 1145a1162.

[10] Lyard F., Lefevre F., Letellier T. and Francis O.; 2006: *Modelling the global ocean tides: modern insights from FES2004*. Ocean Dyn., 56, 394-415, doi:10.1007/s10236-006-0086-x.

[11] McCarthy D.D. and Petit G. (eds); 2003: *IERS Conventions (2003), IERS Technical Note n. 32*. Verlag des Bundesamts für Kartographie und Geodäsie, Frankfurt am Main, Germany, ISBN 3-89888-884-3.

[12] Pilinski M. D., Argrow B. M., Palo S. E., and Bowman B. R., *Semi-Empirical Satellite Accommodation Model for Spherical and Randomly Tumbling Objects*, Journal of Spacecraft and Rockets, Vol. 50, No. 3, 2013, pp. 556571.

[13] Springer T., *NAPEOS mathematical models and algorithms*, tech. rep., DOPS-SYS-TN-0100-OPSGN, 2009.

[14] Visser P.N.A.M., van den IJssel J., van Helleputte T., Bock H., Jäggi A., Beutler G., Svehla D., Hugentobler U. and Heinze M.; 2009: *Orbit determination for the GOCE satellite.* Adv. Space Res., 43, 760-768, doi:10.1016/j.asr.2008.09.016.

[15] Ziebart M., *Generalized analytical solar radiation pressure modelling algorithm for spacecraft of complex shape*, Journal of spacecraft and rockets, Vol. 41, No. 5, 2004, pp. 840848.